

PAPER • OPEN ACCESS

Water Pollution Fiber Sensor Based on Surface Plasmon Resonance Technique; Implementation and Characterization

To cite this article: Maher Khaleel Ibrahim *et al* 2021 *J. Phys.: Conf. Ser.* **1963** 012077

View the [article online](#) for updates and enhancements.

 <p>The Electrochemical Society Advancing solid state & electrochemical science & technology 2021 Virtual Education</p> <p>Fundamentals of Electrochemistry: Basic Theory and Kinetic Methods Instructed by: Dr. James Noël Sun, Sept 19 & Mon, Sept 20 at 12h–15h ET</p> <p>Register early and save!</p>	
--------------------------------------------------------------------------------------------------------------------------------------------------------------------------------------------------------------------------------------------------------------------------------------------------------------------------------------------------------------------------------------------------------------------------------------------	--------------------------------------------------------------------------------------

Water Pollution Fiber Sensor Based on Surface Plasmon Resonance Technique; Implementation and Characterization

Maher Khaleel Ibrahim^{*1}, Shehab A. Kadhim², Nabeil Ibrahim Fawaz³

^{1,3} Department of Physics, College of Science, University of Anbar, Iraq

² Materials Research Directorate, Ministry of Science and Technology, Iraq

* Corresponding author: mkibrahim@uoanbar.edu.iq

Abstract. In this work, a single fiber optic fiber was developed as a water pollution sensor based on the Surface Plasmon Resonance Phenomenon based upon the Mach - Zehender Interferometry (MZI) technology. The sensor submitted was developed to detect water pollutants. The SPR sensors were prepared by coating a golden metallic film which thickness 42 nm on a chemically etched single-mode fiber with a thickness of 20 micrometers, which achieved the best results of sensitivity to water pollution, the results of the high sensitivity of the optical fiber sensor were obtained based on the surface plasmon resonance phenomenon. The experimental results showed high sensitivity, reaching 1315 pm/mol.l⁻¹ for a salty solution with distilled water, 1705 pm/mol.l⁻¹ for the salty solution with tap water, as well as 2222 pm/mol.l⁻¹ for sugar solution with distilled water, and 1925 pm/mol.l⁻¹ for sugar solution with tap water. This means that these sensors which are based on SPR could be very useful in the field of water pollution detection.

Keywords: optical fiber sensors, Surface Plasmon Resonance, evanescent wave, water pollution, MZI.

1. Introduction

Over the past few years, several sensing techniques that can be used to quickly and accurately quantify several physical, biological, and biochemical parameters were thoroughly investigated and these investigations were the first to use surface plasmon resonance (SPR) for chemical sensation. Since then, the SPR sensor concept has been studied [1].

Optical sensors dependent on surface plasmon resonance (SPR) have been highly attracted. These sensors are highly sensitive and enable direct control of biomolecular interactions and biological and chemical reactions as well as changes of 10⁻⁶ refractive index. Metal-coated optic fibers were suggested to create miniaturized SPR sensors as an alternative to bulk setups. The benefit of fiber-based SPR sensors over their large equivalent is lightweight, remote sensing, and multiplexing options[2].

From the previous studies in this field : Cátia Leitãoa, Arnaldo Leal-Juniorb et al in 2021 . The development and feasibility testing of an immune cortisol sensor were presented in this paper. The sensor is based on Surface Plasmon Resonance (SPR) with a golden-palladium (AuPd) alloy coating that uses unclad plastic optical fiber (POF) as a sensation enhancer for SPR. The AuPd coated fibers have been used to monitor the presence of cortisol as a goal



analyzer and have been passivated by the Bovine Serum Albumin (BSA). A change in the refractive index on AuPd's surface, resulting in a shift in the SPR signature wavelength, was caused by the antibody-antigen binding reaction. The cortisol sensor has been measured to measure between 0.005 and 10 ng/mL at different concentrations. A wavelength change of 15 nm was recorded by the biosensor for the test area and a high susceptibility was demonstrated. The proposed POF sensor based on SPR has an affordable method of interrogation, high sensitivity, and low LOD, easy signal processing, and finds significant applications in various biological fields [3].

Huanzhu Lv, Kefei Zhang, et al 2021. A new type of polymethyl methacrylate (PMMA) fiber refractive index sensor is being proposed in this study, extended to the measurement of the liquid refractive index based on surface plasmon resonance (SPR). The SPR theory and structural characteristics of the laterally polished D-type fiber investigate the performance. The effect of a metal film material, the film thickness of the metal, and the sensing area length on the sensor's spectral characteristics are investigated to achieve the optimal parameters of the SPR sensor. The SPR fiber sensor is produced and used for the preparation experiment. The improvement in the glycerol solution's refractive index is identified and evaluated at the 20 °C constant. Experimental findings suggest that the proposed SPR fiber sensor has up to 3328.1 nm/RIU in the 1,334–1,388 range, which can be used as a material for alternative bio-sensing studies.[4]

H. Akafzade, et al 2020 A new type of SPR sensor generated with a multi-layer nanostructure Ag/Si₃N₄/Au is introduced in this study. In measuring the relative concentration of glucose in glucose and water solutions, this sensor has shown excellent results. This work shows that the sensor can overcome the relative glucose concentrations in glucose/water solutions to a maximum of approximately one percent. The sensor output is greatly improved by the high intensity associated with the surface plasmon resonance in the evanescent electric fields [5].

To explain SPR, the phenomenon of total internal reflection of light at the interface between two non-absorbing media should first be described. The light will refract against the interface if a light beam passes through a certain interface from the higher to the lower refractive index medium figure 1a. If the incidence angle changes, the refracted beam is paralleled to the surface: all of the light is reflected beyond that in the medium of the higher refractive index (at higher incidence angles). This is total internal reflection, TIR figure 1 b [6].

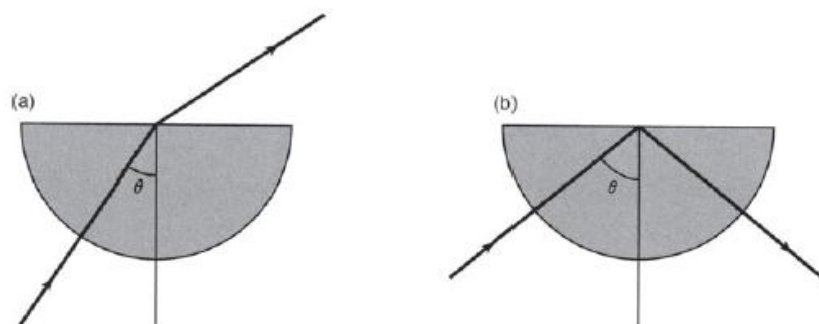


Figure. 1. (a) Light from a denser or less dense medium is refracted to the interface plane. (b) Total internal reflection takes place at and above a critical incidents angle and no light is transferred to a less dense medium [6].

Although this reflected beam does not lose net energy in the interface under TIR conditions it leaks into the medium of the low refractive index an electric field amplitude called the

evanescent wave. The longitude of the evanescent wave of the ground is the same as the incident light. With the increasing distance from the interface, the amplitude of the wave decreases exponentially and decreases over around one light wavelength of the surface [7].

In all cases where total internal reflection occurs, the evanescent field wave appears. However, if the evanescent wave may interfere with a layer of a conductor material such as metal a new phenomenon is created. Now, the P-polarised portion of the evanescent field wave will pervade a metal layer and excite electromagnetic surface waves at the interface with the sample solution. This component is the electric field component lying in the incident plane. These are called surface plasmons, similar to photons which indicate light waves' particle properties [6].

Surface plasmons are oscillations of charge density at an interface between metal and dielectricity. These oscillations get excited as the incident light energy and wave vector at the interface equates to the interface-supported Plasmon surface modes. Due to these oscillations, a wave is formed, called a Surface Plasma Wave, from which the interface, with its field amplitude, exponentially decays, both in the metal and in the dielectric media [8].

The interface of a metal film and a dielectric media (superstrate) at the surface plasmon is excited in SPR sensors which changes in the refractive index to be measured. A change in the superstrate refractive index results in a change in the plasmon surface propagating constant. This alteration changes the coupling state between a light wave and the surface plasmon, a change in one of the properties of the optical wave that interacts with the plasmon surface [2]. SPR sensors are classifiable as SPR sensors with wave spectral, intensity, phase, or polarization modulation based on the characteristics of the light wave interacting with the surface plasmon [9]. In this work, an optical fiber sensor based on SPR and MZI technique is presented. this sensor is used to detect the pollutant in water. the salty and sugary liquids are used as an example of water pollutant.

2. Theory

The SPR sensing is based on Kretschmann's attenuated total reflection principle (ATR). A fiber-core-metal film sensing medium is considered in the optical fiber-based SPR sensor. as shown in figure 2 [1].

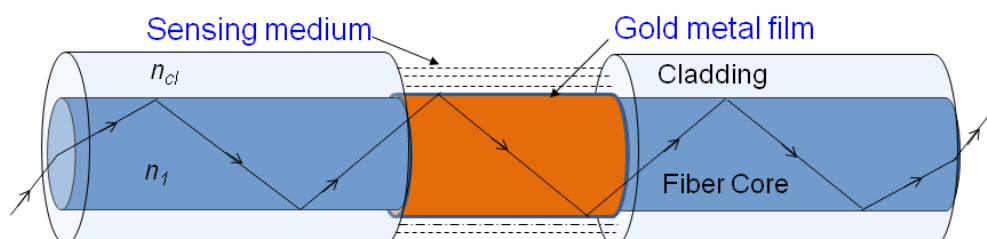


Figure 2. Schematic of a fiber optic SPR sensor [8].

2.1 Layer I (fiber core)

This coating is constructed from fused silica, the basis of the optical fiber. According to the Sellmeier dispersion relation, the refractive index of fused silica change with wavelength as [1]:

$$n_1(\lambda) = \sqrt{1 + \frac{a_1\lambda^2}{\lambda^2 - b_1^2} + \frac{a_2\lambda^2}{\lambda^2 - b_2^2} + \frac{a_3\lambda^2}{\lambda^2 - b_3^2}} \quad (1)$$

where λ is the wavelength in μm and a_1, a_2, a_3, b_1, b_2 and b_3 are Sellmeier coefficients. The values of these coefficients are given as: $a_1 = 0.6961663, a_2 = 0.4079426, a_3 = 0.8974794, b_1 = 0.0684043 \mu\text{m}, b_2 = 0.1162414 \mu\text{m}$ and $b_3 = 9.896161 \mu\text{m}$.

2.2 Layer II (metal film)

There is a metal layer. The dielectric constant of every metal is calculable based on the Drude model [10]:

$$\varepsilon_m(\lambda) = \varepsilon_{mr} + i\varepsilon_{mi} = 1 - \frac{\lambda^2\lambda_c}{\lambda_p^2(\lambda_c + i\lambda)} \quad (2)$$

Here, λ_p and λ_c are the plasma wavelength and the collision wavelength of the metal, respectively. $\lambda_p = 1.6826 \times 10^{-7} \text{ m}, 1.4541 \times 10^{-7} \text{ m}, 1.3617 \times 10^{-7} \text{ m}, 1.0657 \times 10^{-7} \text{ m}$ and $\lambda_c = 8.9342 \times 10^{-6} \text{ m}, 1.7614 \times 10^{-5} \text{ m}, 4.0852 \times 10^{-5} \text{ m}, 2.4511 \times 10^{-5} \text{ m}$ for Au, Ag, Cu, Al metals respectively.

2.3 Layer III (sensing medium)

The layer consists of a medium for sensing. The sensing medium dielectric constant is ε_s . If n_s is the refractive index of the sensing medium, then $\varepsilon_s = n_s^2$. The resonance condition for the excitation of surface plasmon wave is given as [1]:

$$\frac{2\pi}{\lambda} n_1 \sin \theta = \text{Re}\{K_{sp}\} \quad (3)$$

Where

$$K_{sp} = \frac{\omega}{c} \sqrt{\frac{\varepsilon_m \varepsilon_s}{\varepsilon_m + \varepsilon_s}} = \frac{2\pi}{\lambda} \sqrt{\frac{\varepsilon_m n_s^2}{\varepsilon_m + n_s^2}} \quad (4)$$

is the surface plasmon propagation constant and c is a vacuum speed of light. The left-hand side of equation 3 denotes the propagation constant of the light incident at an angle θ and the right-hand side shows the real part of the propagation constant of the surface plasmon.

3- Experimental work

The experiment was performed with a section of the commercial SMF with core diameters $125 \mu\text{m}$ and $9 \mu\text{m}$. It was stripped and washed very well about 3 cm long in the middle area of SMF. After this part was immersed in Hydrofluoric acid (HF) that is, its diameter was reduced to the desired value and chemically etched. The concentration of HF acid before dilution was 48%, this strong acid had been diluted with distilled water as a ratio of (1 mm³ HF: 1 mm³ distilled water). The etching process took place at room temperature and the required cladding diameter has been achieved at an etching time off 150 min. The $20 \mu\text{m}$ thickness of the cladding was obtained through its time.

The Magnetron Sputtering plasma System was used to spray the optical fiber previously etched with gold. The Coating process took the time 15 minutes.

The Fizeau fringe method (The Fizeau interferogram was obtained by the Tolansky or Michelson techniques) had been used in this work to measure the thickness of the gold, and the 42 nm was obtained thickness.

Figure 3, illustrates the scheme of the experiment. The light source was a single-mode diode laser (Thorlabs) with a central wavelength of 1550 nm, and 1.5 mW power was connected to the input arm of a 1x2 optical coupler. By using a splitter (OC1. 1x2 50% 50%), the light transmitted through the fibers was divided into two intensities of equal value between the two optical fibers. The sensor arm was immersed in liquids that had been polluted. Both arms were then collected using another optical 2x1 coupler (OC2). The output port was connected to the Optical Spectrum Analyzer (THORLABS OSA 203), which had a wavelength range of

1000 to 2600 nm and a resolution of 0.1 nm, and to the OSA, which was connected to the computer using software supplied by Thorlabs OSA.

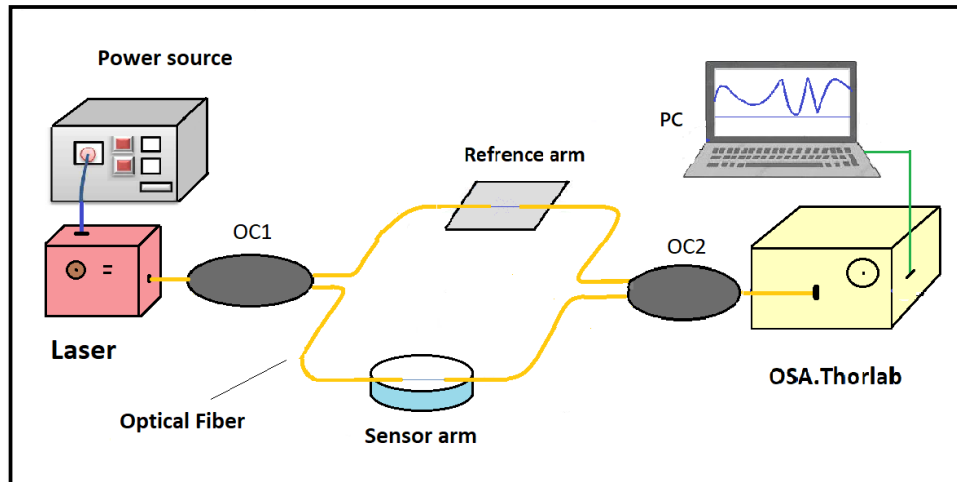


Figure 3. Experimental set-up of water pollution sensor based on SPR technique

The medium adjacent to the surface of the plasmonic metal is considered the medium of the sensor. Different sodium chloride and sugar solution concentrations of water have different refractive indexes to be used as a sensor medium. We considered salt and sugar solutions as an indicator of water contamination in this study because of the great effect on the environment of increasing their concentration in the water.

The tested solutions of sodium salt (NaCl) and Sugar ($C_{12}H_{22}O_{11}$) were prepared at different concentrations using the following equation[11] :

$$C = \frac{m}{V} \times \frac{1}{MW} \quad (5)$$

Where C is the molar concentration in mol/L (Molar or M). This is also referred to as molarity, m is the mass (i.e., weight) of solute in grams (g) that must be dissolved in volume V of the solution to make the desired molar concentration (C) and MW is the molecular weight in g/mol (MW NaCl = 58.4428 g/mol, MW $C_{12}H_{22}O_{11}$ = 342.30 g/mol).

water pollutions samples are prepared with different concentrations ranging from 0.05 mol/liter to 0.45 mol/liter of sodium chloride salt and sugar by dissolving them separately in distilled water and tap water As shown in table (1).

Table 1. The Concentration of the Salty and Sugary Solution.

Wt. NaCl gm in 40ml H ₂ O	Wt. C ₁₂ H ₂₂ O ₁₁ gm In 40ml H ₂ O	Const. Mol/Liter
0.1168	0.648	0.05
0.3504	2.052	0.15
0.584	3.42	0.25
0.8176	4.788	0.35
1.0512	6.156	0.45

Firstly, the spectrum is recorded without any liquid in the air surrounding the sensing area as a reference spectrum. Then the sensing optical fiber is immersed in solutions with different concentrations and different refractive indices or a sample solution is dropped on the sensor's metal-coated face and the spectrum was recorded by OSA.

4 - Results and Discussion

The experiment was carried out on an optical fiber sensor arm with a thickness of 20 μm , after coating it with gold metal to the required thickness 42nm and immersing it in salty and sugary liquids at various concentrations. OSA was used to collect and analyze the transmission spectrum. With a scan time of 30 sec, the fiber output was registered. The following results were obtained in determining the sensitivity of the optical fiber while increasing the concentration of the solution by performing mathematical and algebraic operations using a software optical spectrum analyzer. And as mentioned, salty and sugary solutions will be used with distilled water and tap water. The test will be started with the Salty and Sugary Solution in distilled water.

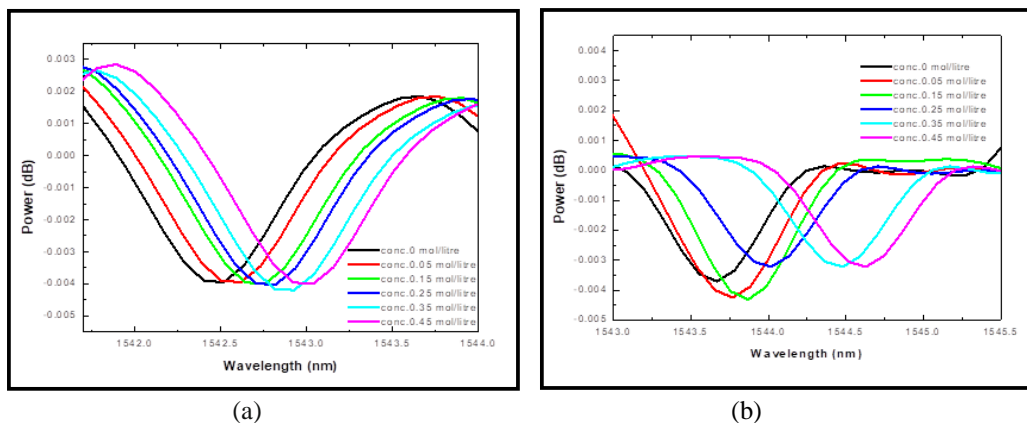


Figure 4. The SPR spectrum of the optical fiber sensor from const. (0 to 0.45) mol/liter. (a) for the salty solution with distilled water (b) for the sugary solution with distilled water

The spectra are obtained by using OSA to record the light transmission curves through the optical fiber. The SPR curve is a wavelength curve that has a sharp dip at a specific wavelength called the resonance wavelength λ_{res} . The location of this dip is determined by the sensing medium's refractive index.

The SPR spectrum for an optical fiber sensor with a gold thin film of thickness 42 nm is shown in Figure 5. It should be noted that each curve has a deep at a certain wavelength defined as the resonance wavelength (λ_{res}). If the refractive index or concentration of the solution increases, the resonance wavelength becomes longer.

"The change in the resonance wavelength per unit of the refractive index" is how the fiber-based configuration of an SPR sensor (S_n) [12]. If the shift is large, sensitivity is large. As shown in Figure 5 and table 2, The resonance wavelength changes by λ_{res} if the refractive index of the sensing layer is changed by δn . With spectral interrogation, an SPR sensor's sensitivity (S_n) is described as [12] :

$$S_n = \frac{\delta \lambda_{\text{res}}}{\delta n} \quad (6)$$

Table 2. The value of the resonance wavelengths according to the spectrum of Salty and Sugary Solution with distilled water from Const. (0- 0.45) mol/liter

Const. mol/liter	Resonance wavelength λ_{res} (nm) Salty Solution	Resonance wavelength λ_{res} (nm) Sugary Solution
0	1542.45	1543.638
0.05	1542.58	1543.736
0.15	1542.731	1543.84
0.25	1542.88	1544.01
0.35	1542.92	1544.448
0.45	1543	1544.617

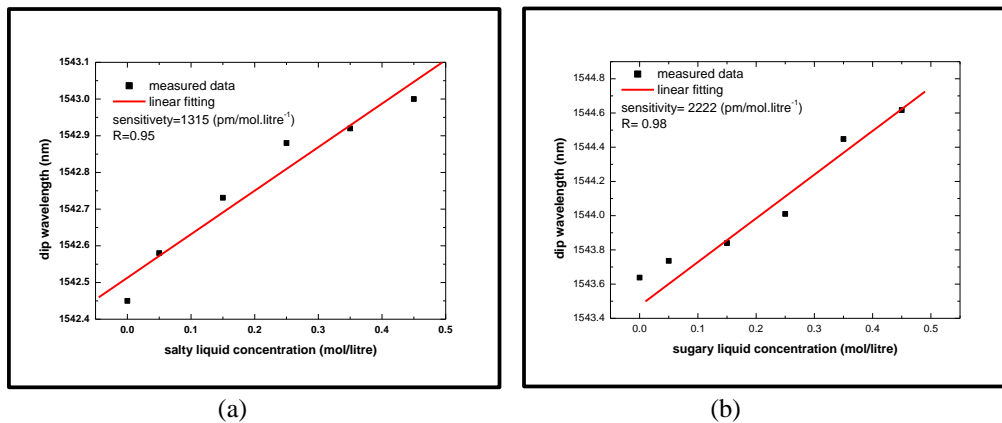


Figure 5. The relationship of wavelength resonance with liquid concentration for (a) salty solution (distilled water). (b)sugary solution (distilled water)

In Figure 6, λ_{res} are plotted as a function of refractive index or concentration to measure the sensitivity, The sensor's sensitivity is determined by the slope of this straight line. when using Salty and Sugary Solution with Tap Water the following result was obtained, table 3 summarized the above results.

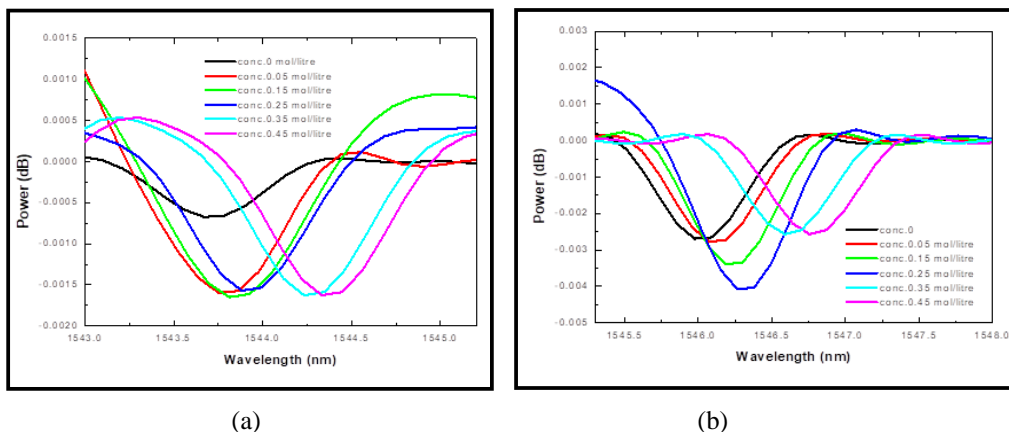
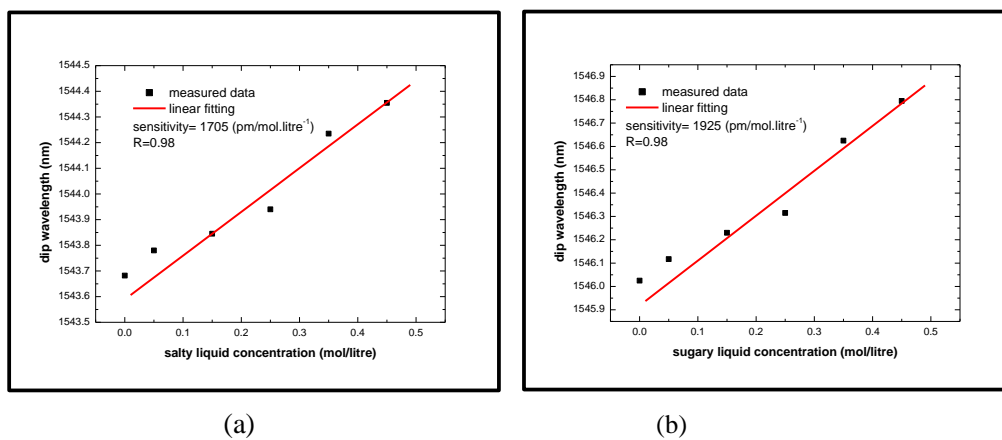


Figure 6. The SPR spectrum of the optical fiber sensor from Const. (0 to 0.45) mol/liter. (a) for the salty solution with tap water (b) for the sugary solution with tap water.

Table 3. Value of the resonance wavelengths according to the spectrum of Salty and Sugary Solution with tap water from Const. (0- 0.45) mol/liter

Const. mol/liter	Resonance wavelength λ_{res} (nm) Salty Solution	Resonance wavelength λ_{res} (nm) Sugary Solution
0	1543.682	1546.025
0.05	1543.78	1546.117
0.15	1543.845	1546.23
0.25	1543.94	1546.315
0.35	1544.235	1546.625
0.45	1544.355	1546.795

**Figure 7.** The relationship of wavelength resonance with liquid concentration for (a) salty solution (tap water). (b)sugary solution (tap Water)

Through the figures 4 and 6 where the spectra are obtained by recording the curves of light propagation across optical fibers through OSA, which is known as the SPR curve, we find a sharp dip in λ_{res} at a particular wavelength called resonance wavelength λ_{res} . The location of this dip is determined by the sensing medium's refractive index or concentration. We can also observe for two different refractive indices of the superstrate, the intensity of a light wave interacting with a surface plasmon as a function of wavelength. The phenomenon of surface plasmon resonance, which contributed greatly to the increase in optical fiber sensitivity, is the reason for this, as we can see through the figures 5 and 7 where the sensitivity of the optical fiber reached 1315 pm/mol.litre⁻¹ when the salt concentration in distilled water changed and 2222 pm/mol. liter⁻¹ when changing the concentration of sugar in distilled water. Also, concerning Salty and sugary solutions with tap water, the sensitivity of optical fibers reached and to 1705 pm/mol. liter⁻¹ when changing the concentration of the salty solution in tap water and to 1925 pm/mol. liter⁻¹ when the concentration of the sugary solution changed in tap water.

So that SPR is explained, a new effect occurs as an evanescent wave interacts with an abstract material layer like metal. A non-magnetic metal, such as gold, is polarized by surface plasmons, creating a more evanescent wave field when spreading across the surface of the metal film. This enhanced wavefield penetrates the medium for a short distance, like the evanescent wavelength produced by total internal reflection at a non-coated interface.

It is important first to understand the resonance phenomenon in SPR. The plasmon wave is confined to the metal layer on the interface plane. Several factors affect the wave momentum, including the structure and thickness of the metal layer. It is only when the incident light vector's energy and momentum match the surface plasmons' energy and momentum that plasmons form in the metal layer [6].

5. Conclusions

In this work, the performance characteristics of an optical fiber sensor based on surface plasmon resonance had been submitted. This fiber had been designed for water pollution purposes. To further improve the performance and to employ the phenomenon of surface plasmon resonance, the optical fiber with a thickness of 20 μm was sprayed with gold and a thickness of 42 nm. We found that there is an optimal film thickness 42 nm. Fibers with a smaller cladding diameter and optimal film thickness would also be more ideal for the design and development of sensors. The results of a detailed experimental study indicate that the properties of the film regulated by the detector, as well as the diameter of the fiber cladding, play a significant role in obtaining the highest sensitivity. A chemically-etched single-mode fiber SPR sensor was demonstrated. The experimental results showed high sensitivity, reaching 1315 $\text{pm}/\text{mol}\cdot\text{l}^{-1}$ for a salty solution with distilled water, 1705 $\text{pm}/\text{mol}\cdot\text{l}^{-1}$ for a salty solution with tap water, as well as 2222 $\text{pm}/\text{mol}\cdot\text{l}^{-1}$ for sugar solution with distilled water, and 1925 $\text{pm}/\text{mol}\cdot\text{l}^{-1}$ for sugar solution with tap water.

Thus it can be concluded that the sensor sensitivity and performance parameters of a single-mode optical fiber of 20 μm cladding diameter and coated with a 42 nm gold layer have been improved and it appears that the experimental implementation of gold as a thin film coated is a good response.

As it clears above the submitted sensor has high sensitivity and linearity in spite of low pollutant concentrations its success to detect the minor pollutant in water samples. So this type of sensors could be a very good choice in chemical and environmental applications.

References

- [1] Sharma NK. 2012. Performances Of Different Metals In Optical Fibre-Based Surface Plasmon Resonance Sensor. *Pramana - J Phys.*;78(3):417–27.
- [2] Monzón-Hernández D, Villatoro J, Talavera D and Luna-Moreno D. 2004. Optical-Fiber Surface-Plasmon Resonance Sensor With Multiple Resonance Peaks. *Appl Opt.*;43(6):1216–20.
- [3] Leitão C, Leal-Junior A, Almeida AR, Pereira SO, Costa FM, Pinto JL, et al. 2021. Cortisol Aupd Plasmonic Unclad POF Biosensor. *Biotechnol Reports.*;29.
- [4] Lv H, Zhang K, Ma X, Zhong W, Wang Y and Gao X. 2021. Optimum Design Of The Surface Plasmon Resonance Sensor Based On Polymethyl Methacrylate Fiber. *Phys Open.*;6(July 2020):100054.
- [5] Akafzade H, Hozhabri N, Sharma SC. 2021. Highly Sensitive Plasmonic Sensor Fabricated With Multilayer Ag/Si3N4/Au Nanostructure For The Detection Of Glucose In Glucose/Water Solutions. *Sensors Actuators, A Phys.*;317:112430.
- [6] Markey F. 1 . Principles of Surface Plasmon.
- [7] Thompson NL, Lagerholm BC. 1997. Total Internal Reflection Fluorescence: Applications In Cellular Biophysics. *Curr Opin Biotechnol.*;8(1):58–64.
- [8] Srivastava SK. 2014. Fiber Optic Plasmonic Sensors: Past, Present and Future. *Open Opt J.*;7(1):58–83.
- [9] Republic C. 2006. Surface Plasmon Resonance (SPR) Sensors.;(July):45–67.
- [10] Ordal MA, Long LL, Bell RJ, Bell SE, Bell RR, Alexander RW, et al. 1983. Optical Properties Of The Metals Al, Co, Cu, Au, Fe, Pb, Ni, Pd, Pt, Ag, Ti, And W In The

- Infrared And Far Infrared. *Appl Opt.*;22(7):1099.
- [11] Kaufman M. 2006. Principles of Thermodynamics. Integration of Alternative Sources of Energy.. 28–56 p.
- [12] Perhirin S, Auffret Y. 2013. A Low Consumption Electronic System Developed For A 10km Long All-Optical Extension Dedicated To Sea Floor Observatories Using Power-Over-Fiber Technology And SPI Protocol. *Microw Opt Technol Lett.*;55(11):2562–8.